(AUTOMATIC) TARGET DETECTION IN SYNTHETIC APERTURE RADAR IMAGERY VIA TERRAIN RECOGNITION

R. Paget, J. Homer[*]

Dept. Comp. Science and Elec. Engineering
University of Queensland
QLD, Australia

D. Crisp[†]

Surveillance Systems Division
Defence Science Technology Organisation
Salisbury, SA, Australia

ABSTRACT

Surveillance of large areas of the Earths surface is often undertaken with low resolution synthetic aperture radar (SAR) imagery from either a satellite or a plane. There is a need to process these images with automatic target detection (ATD) algorithms. Typically the targets being searched for are vehicles or small vessels, which occupy only a few resolution cells. Simple thresholding is usually inadequate for detection due to the high amount of noise in the images. Often the background has a discernible texture, and one form of detection is to search for anomalies in the texture caused by the presence of the target pixels. To perform this task a texture model must be able to model a variety of textures at run time, and also model these textures well enough to detect anomalies. We accomplish this with our multiscale nonparametric Markov random field (MRF) texture model.

1. INTRODUCTION

Defence reviews of Australia [1, 2] have consistently identified the need for airborne surveillance of remote areas and coastlines of Australia. A specific requirement is for airborne surveillance based on synthetic aperture radar (SAR) imagery and automatic processing of the imagery as it is being formed [1]. With current resolving powers, and with vast areas of terrain, modern SAR sensors can produce large quantities of imagery in a short space of time. The large amount of data requiring real time processing means that a computer system is needed to perform the searches for any incursions, or in other words perform ”automatic target detection” (ATD). From previous work, it has been made clear that no single algorithm will suffice, and that new approaches need to be continually sought [3].

An advantage of using SAR imagery is that it is not impeded by cloud cover, however the resolution is lower than that which can be obtained from a photographic imaging system. In low resolution synthetic aperture radar (SAR) imagery, targets of interest may only be a few image pixels in size, and may be buried in radar clutter plus terrain texture. Conventional target detection by radar requires the target to have a much stronger signal than the background texture and noise, thus allowing a simple thresholding process to extract the target from the background. However the nature of the noise associated with SAR, called “speckle”, makes thresholding very susceptible to high levels of false target detection. Current target detection algorithms have been criticised for their very high false detection rates [3].

In the current literature there are two methods for reducing the false detection rate. Firstly, the detection algorithm itself can be designed to detect anomalies in the background texture caused by the presence of the target pixels [4, 5]. The second method for reducing the false detection rate is based on segmenting the image into homogeneous texture regions prior to detection. It has been shown that by restricting the standard constant false alarm-rate receiver (CFAR) detectors to homogeneous texture regions, detection performance can be improved [6].

One possibility for improving the false detection rates is to use a better texture model. We believe that our texture model [7] will do just that by giving a better statistical understanding of the background texture. In [7, 8], we demonstrated the ability of the texture model to fully characterise a multitude of different textures by using the model to synthesise visually similar texture with regard to a set of training textures, as shown in Fig. 1.

For a texture model to detect anomalies in different types of texture, it not only has to model the texture well, but also be able to delineate between similar texture and significantly different texture. In [9, 10] we showed the potential for our model to be used in our unique classification method called “open-ended” classification. Unlike other texture classification methods, our method does not require an extensive library of predefined textures to perform nearest neighbour type measurements. Instead our new classification method uses the underlying characteristics of the texture to perform a goodness-of-fit type measurement. Basically we are able to identify specific textures from a suite

[*] Thanks to CSSIP agency for funding.

[†] The third author performed the work while at DSTO.

(a) (a.1) (b) (b.1) (c) (c.1)

Fig. 1. Synthesised VisTex textures using a nonparametric multiscale MRF model with a 7×7 neighbourhood. The VisTex textures are: (a) Bark.0003; (b) Food.0010; (c) Leaves.0016. The larger images are the synthesised textures

of textures for which predefined models do not exist. This is a significant advance on all other types of texture classification schemes, and is what is required to find texture anomalies.

2. NONPARAMETRIC MULTISCALE MRF MODEL

The nonparametric multiscale MRF model, as presented in [7, 8], is based on probability density estimation of a multi-dimensional histogram. This multi-dimensional histogram is produced from recording the frequency of a set of grey level co-occurrences between a pixel and its neighbours, which are defined through a neighbourhood. The size of the neighbourhood determines the dimensionality of the histogram. The estimated probability function over this histogram is called the local conditional probability density function (LCPDF).

The domain of the multi-dimensional histogram domain is equal to the number of different grey levels in the image to the power of the number of neighbours in the neighbourhood. With a regular 3×3 neighbourhood, and 256 grey levels, a 512×512 homogeneously textured image would only fill $E-15\%$ of the domain space. This means that there is very little data to produce a proper LCPDF. When the sample data is sparsely and thinly dispersed over its domain (as in our case), nonparametric estimates of the probability function tend to be more reliable than their parametric counterparts if the true underlying distribution is unknown [11]. This is one reason why we have opted to use the nonparametric multiscale MRF model. Another reason is that we can arbitrarily vary the statistical order of the model while not being restricted by an underlying parametric function.

To test the ability of our texture model to adequately model arbitrary textures, we used our model to synthesise various natural textures. The synthesise algorithm is formalised in [8]. In Fig. 1 128×128 training textured images were used to synthesise 256×256 synthetic textured images. A subjective comparison of the training and synthetic textured images shows that the nonparametric multiscale MRF model is able to capture the unique characteristics of the training textures.

3. OPEN-ENDED TEXTURE CLASSIFICATION

To identify a target we will look for anomalies in the background texture for which we will use our open-ended texture classifier [9, 10]. Open-ended texture classification is performed by identifying a population of statistics that uniquely identifies a particular texture and making a goodness-of-fit comparison between it and an unknown texture. As our nonparametric multiscale MRF model is able to synthesise highly representative textures of a training texture, we are able to say that the respective LCPDF contains information that is unique to that texture. By comparing the population of probabilities that are obtained by placing the LCPDF over the background texture to the population of probabilities that are obtained by placing the LCPDF over the target texture, we are able to perform a goodness-of-fit test between the two populations. If the goodness-of-fit is significantly high then we can say that the target texture is that of the background texture and is not a target.

4. TARGET DETECTION

For target detection we have slightly modified the open-ended texture classifier. First, the classifier is being used on pre-segmented images of possible targets, as displayed in Figs. 2 and 3. This ground truthed data consists of 76032 45×45 images where the possible target is in the middle of each image. Of these images only 0.5% have true targets. The aim of algorithm is to dramatically reduce the number of false targets, while retaining close to all of the true targets. Since we know that the target is in the middle of each image, we define the target region as being in the middle and everything else as background texture.

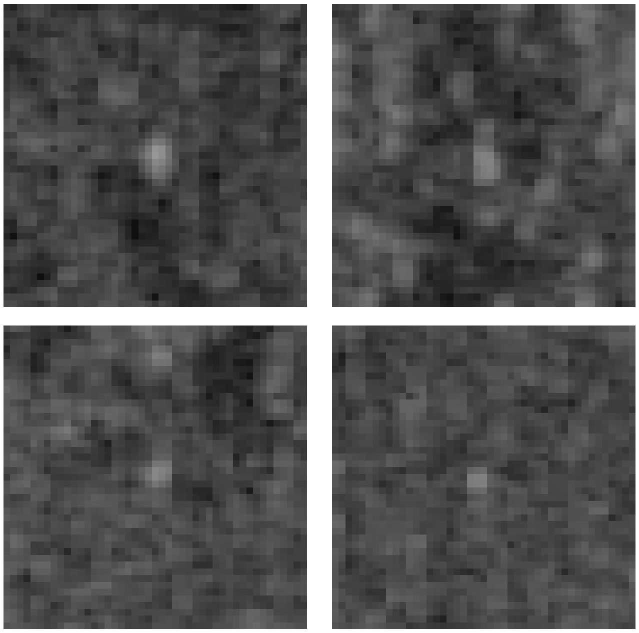

Fig. 2. True targets displayed in the centre of these 4 SAR image segments.

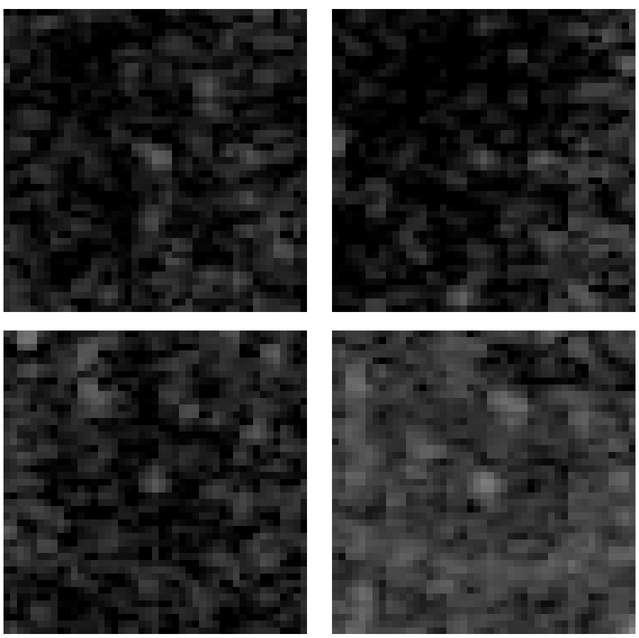

Fig. 3. False targets displayed in the centre of these 4 SAR image segments.

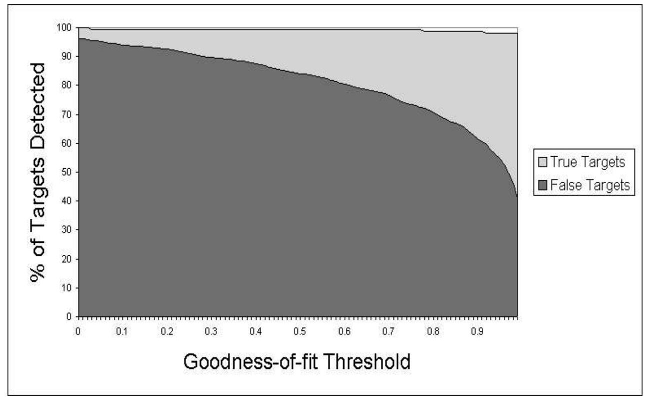

Fig. 4. The percentage of targets detected for MRF model n1c0t0w6.

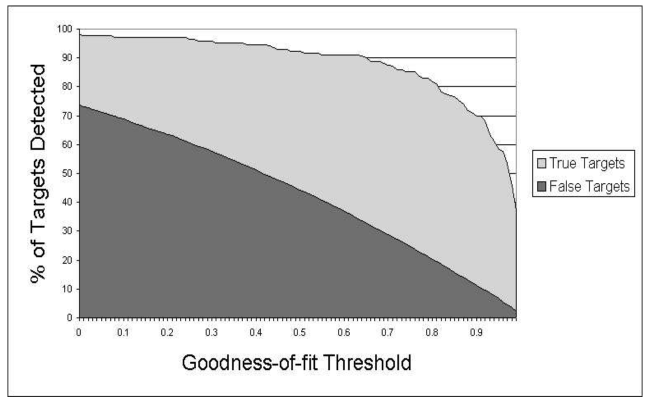

Fig. 5. The percentage of targets detected for MRF model n3c2t1w4.

Second, in defining the LCPDF of the multi-dimensional histogram, we found that we got the best results if we did not use the Gaussian kernel function, but simply a minimum distance measure, as described in [7]. The most likely reason for this failure of Gaussian kernel function would be an inability to find the appropriate window width or smoothing parameter [11]. Not using one at all was better than using the wrong window width.

Third, we modified the open-ended texture classifier by improving the way multiple sets of probability characteristics were combined. In [7] we simply did a goodness-of-fit test for each set of probability characteristics, and then added the results to obtain an overall result. In this paper we did a two pass approach. One to get the probability characteristics for each clique and quad-tree level. Then a second pass to get the probability of obtaining the specified set of probability characteristics for each pixel. Finally the goodness-of-fit test was done on the resulting probabilities for each pixel in the texture.

Table 1. Maximum Separation of True from False Targets

MRF Model	*% True Targets*	*% False Targets*	*Difference*
n1c0t0w2	95.7831	49.1141	46.6690
n1c0t0w4	98.1818	48.6900	49.4918
n1c0t0w6	98.1818	40.8977	57.2841
n1c0t1w2	61.9171	32.1006	29.8165
n1c0t1w4	81.8653	37.4280	44.4373
n1c0t1w6	81.3472	35.1727	46.1745
n1c2t0w2	100.0000	87.5660	12.4340
n1c2t0w4	100.0000	85.7598	14.2402
n1c2t0w6	100.0000	74.9797	25.0203
n1c2t1w2	53.2951	32.8751	20.4200
n1c2t1w4	69.2308	18.2420	50.9888
n1c2t1w6	76.3533	29.2877	47.0656
n3c0t0w2	96.0784	56.3422	39.7362
n3c0t0w4	99.3421	68.5711	30.7710
n3c0t0w6	98.6842	63.9889	34.6953
n3c0t1w2	54.9479	21.6457	33.3022
n3c0t1w4	72.9167	23.5184	49.3983
n3c0t1w6	92.4479	57.3799	35.0680
n3c2t0w2	100.0000	98.1185	1.8815
n3c2t0w4	100.0000	98.3405	1.6595
n3c2t0w6	100.0000	93.7550	6.2450
n3c2t1w2	54.7059	23.6806	31.0253
n3c2t1w4	81.1765	19.4171	61.7594
n3c2t1w6	88.3721	35.5536	52.8185

Figs. 4 and 5 show the goodness-of-fit output for two different MRF models. The key to the models is as follows: 'n' refers to the neighbourhood, 1 for nearest neighbourhood and 3 for 3×3 neighbourhood; 'c' refers to the clique size, 0 for no cliques and 2 for pairwise cliques; 't' refers to the quad-tree height, 0 for just original image, and 1 for level 0 and 1 of the image quad-tree; 'w' refers to size of size target region, 2 for a 2×2 region *etc.*

From table 1 it is clear that, at their best goodness-of-fit threshold, the models n1c0t0w6 and n3c2t1w4 gave the greatest discrimination between recognising true targets and removing false targets. However it is model n1c0t0w6 that retained the greatest percentage of true targets of 98% while removing nearly 60% of the false targets.

5. CONCLUSION

Current target detection algorithms for SAR images suffer greatly from too many false detections. As a step towards improving the detection rates, we have proposed using our open-ended texture classifier. Target detection is achieved by modelling the background texture and determining the goodness-of-fit between the target and the background texture. Targets are detected if the goodness-of-fit is low. Using this method we were able to greatly reduce the number of false targets while retaining nearly all of the true targets.

6. ACKNOWLEDGEMENT

The authors would like to acknowledge the Surveillance Systems Division of the Defence Science and Technology Organisation, Australia, for providing the SAR imagery.

7. REFERENCES

[1] *Australian Defence Projects Directory,* Yaffa Publishing, 3rd edition, 1997.

[2] K. Beazley, *The Defence of Australia*, Australian Government Publishing Service, 1987.

[3] IEEE Transactions on Image Processing, *Special Issue on Automatic Target Recognition*, vol. 6, IEEE Signal Processing Society, 1997.

[4] H. Guillemet, H. Benali, F. Preteux, and R. Di Paola, “Noisy fractional Brownian motion for detection of perturbations in regular textures,” *Statistical and Stochasic Methods for Image Processing*, vol. Proceedings of SPIE 2823, pp. 40–51, 1996.

[5] L. M. Kaplan and R. Murenzi, “Evaluation of cfar and texture based target detection statistics on sar imagery,” in *Proceedings of ICASSP'98*, 1998, pp. 2141–2144.

[6] I. McConnell and C. Oliver, “Segmentation–based target detection in sar,” *SAR Image Analysis, Modelling and Techniques II*, vol. Proceedings of SPIE 3869, pp. 45–54, 1999.

[7] Rupert Paget, *Nonparametric Markov random field models for natural texture images,* Ph.D. thesis, University of Queensland, St Lucia, QLD Australia, Dec. 1999.

[8] Rupert Paget and Dennis Longstaff, “Texture synthesis via a noncausal nonparametric multiscale Markov random field,” *IEEE Transactions on Image Processing*, vol. 7, no. 6, pp. 925–931, June 1998.

[9] Rupert Paget and Dennis Longstaff, “Nonparametric markov random field model analysis of the meastex test suite,” in *International Conference on Pattern Recognition*, Barcelona, Spain, Sept. 2000, IAPR, vol. 3, pp. 939–942.

[10] Rupert Paget and Dennis Longstaff, “Open–ended texture classification for terrain mapping,” in *International Conference on Image Processing*, Vancouver, Canada, Sept. 2000, IEEE Signal Processing Society, vol. 3, pp. 584–587.

[11] B. W. Silverman, *Density estimation for statistics and data analysis,* Chapman and Hall, London, 1986.